Materials Today Communications 27 (2021) 102434

Contents lists available at ScienceDirect

Materials Today Communications

journal homepage: www.elsevier.com/locate/mtcomm

Upconversion and cooperative luminescence in YBO_3:Yb^{3+}- Er^{3+}

F. Rivera-López [a,*], M.E. Torres [b], G. Gil de Cos [b]

[a] Departamento de Ingeniería Industrial, Escuela Superior de Ingeniería y Tecnología, Universidad de La Laguna, Apdo. 456. E-38200 San Cristóbal de La Laguna, Santa Cruz de Tenerife, Spain

[b] Departamento de Física, Universidad de La Laguna, Apdo. 456. E-38200 San Cristóbal de La Laguna, Santa Cruz de Tenerife, Spain

ARTICLE INFO

Keyword:
Borate (YBO_3)
Yb^{3+}-Er^{3+}
Upconversion
Cooperative luminescence

ABSTRACT

This paper reports the frequency upconversion and cooperative luminescence in YBO_3:Yb^{3+}-Er^{3+} sample. After cw diode laser excitation, at 980 nm, three clear bands were observed at around 650, 545 and 484 nm, corresponding to red, green and blue emissions, respectively. The bands centred at 650 and 545 nm can be attributed to upconversion emissions from Er^{3+} ions. Mechanisms of energy transfer upconversion and excited-state absorption of pump radiation are proposed in order to explain these radiative transitions. The blue emission at 484 nm is analysed with the aim to elucidate if it can be attributed to cooperative luminescence from Yb^{3+}-pairs. Finally, the color diagram is presented so as to study the color purity of the sample.

1. Introduction

Synthesis and luminescent properties of rare earth borates, denoted as $REBO_3$, have been widely investigated during recent years. Among these compounds, yttrium borates (YBO_3) doped with trivalent rare earth (RE^{3+}) ions have been intensively studied for different applications, for example, Hg-free fluorescent lamps, plasma display panels (PDPs) [1–3], solar cells [4,5] or waveguide thin films [6]. YBO_3 have attracted much attention due to their good chemical and thermal stability, easy synthesis, low toxicity, wide band gap, excellent optical damage threshold, good maintenance [7,8], high ultraviolet (UV) (200–400 nm) transparency, strong vacuum ultraviolet (VUV) absorption and high luminescent efficiency under VUV excitation (100−200 nm) from Xe/He gas plasma. With respect to the synthesis, various chemical techniques have been developed looking for high quality compounds. Some of these techniques involve solid-state reactions [9], glycothermal methods [10], combustion synthesis [11], hydrothermal methods [12–14], spray-pyrolysis [15], high temperature ball milling [16], precipitation [17], electrochemical deposition [18] or sol-gel [6,19].

The majority of studies are focused on increasing the photoluminescence quality and, in this sense, YBO_3 is considered a particularly useful host lattice for the luminescence of RE^{3+} ions. It is well known that RE^{3+} ions present f–f energy level transitions in a broad range of emission wavelengths. Among these systems, YBO_3:Eu^{3+} is one of the most studied due to its usefulness as an orange-red phosphor [20,21] for PDPs. Other examples are the YBO_3:Ce^{3+} phosphor whose interest is related to the blue emitting luminescence [22] and the YBO_3:Tb^{3+} system due to its potentiality as a green phosphor [23,24]. Furthermore, RE^{3+} co-doped samples, such as the YBO_3:Tb^{3+}-Eu^{3+} system, have been researched to make white light emitting diodes [25], and RE^{3+} tri-doped such as the YBO_3:Tb^{3+}-Eu^{3+}-Dy^{3+} phosphor, which is capable of producing white light by combining blue, green, yellow, orange and red emissions when excited at 365 nm UV light [26].

Among RE^{3+} ions, Yb^{3+} and Er^{3+} have been intensively studied due to their good optical properties. In the case of Yb^{3+} ions, the simple levels configuration, consisting only of two manifolds, the $^2F_{7/2}$ ground state and the $^2F_{5/2}$ upper level, with a typical energy separation of about 10,000 cm^{-1} [27], reveals some advantages, for example, a superior energy storage capability associated to the long lifetime of the excited $^2F_{5/2}$ level. The broad and strong absorption band spectra, at about 980 nm, makes it suitable for tuneable diode excitation. These systems can easily be pumped by commercially available laser diodes. Thus, in compounds where Yb^{3+} ions are forming clusters, cooperative luminescence at around 500 nm is possible [28]. With respect to the Er^{3+} ion, one of the greatest interests concerns the upconversion mechanism, in which lower energy light, usually near-infrared (NIR) or infrared (IR), is converted into higher energies, UV or visible emissions [29]. With respect to upconversion, the Er^{3+} ion is one of the most efficient active center due to its favourable energy level structure. Optical properties can be enhanced by combining different RE^{3+} species via interaction mechanisms among ions. Some ions can be photon pumped, acting

* Corresponding author.
E-mail address: frivera@ull.es (F. Rivera-López).

https://doi.org/10.1016/j.mtcomm.2021.102434
Received 21 October 2020; Received in revised form 4 May 2021; Accepted 4 May 2021
Available online 8 May 2021

efficiently as sensitizers and transferring their excitation to a neighbouring acceptor ion. In this sense, in Er^{3+}-Yb^{3+} co-doped materials, the incorporation of Yb^{3+} ions can lead to an increase of the Er^{3+} luminescence. The strong absorption at 980 nm of Yb^{3+} ions mentioned before and the large spectral overlap between the Yb^{3+} emission and the Er^{3+} absorption are responsible for the efficient energy transfer between both ions, with a significant increase in the upconversion emission [30].

In previous work [31], polycrystalline of pure and Er^{3}-Yb^{3+} co-doped YBO_3 samples were synthesized and characterized by X-ray diffraction (XRD) and Second Harmonic Generation (SHG) experiments. XRD allows the conclusion of a crystal structure according to a non-centrosymmetric space group (C2). On top of that, the existence of an intense SHG was observed in both matrix after pulsed laser excitation, in good agreement with the XRD pattern analysis. In this paper, IR to visible energy upconversion associated to Er^{3+} ions, and cooperative processes related to Yb^{3+} ions, are studied in order to explain the origin of the emissions. Cooperative luminescence is interpreted from measurements of lifetimes and cooperative emission. Thus, chromaticity coordinates are calculated and represented in the color diagram.

2. Experimental

High purity crystalline powder samples of YBO_3 and $Er_{0.1}Yb_{0.1}Y_{0.8}BO_3$ were synthesized by solid-state reaction. The starting materials were Y_2O_3 and H_3BO_3 and Er_2O_3, Yb_2O_3 for the doped compound with 99.99 % purity in adequate proportion. The Er_2O_3, Yb_2O_3 and Y_2O_3 powders were preheated at 600 °C for 5 h. The preheated powders were then weighed, mixed, ground and pressed into pellets for heat treatment at 850 °C into a platinum crucible for 48 h.

Upconversion and cooperative emissions spectra were measured by exciting the sample with a commercial continuous-wave (cw) laser diode at 980 nm. The luminescence of the RE^{3+} ions was focused onto a 0.18 m focal length single-grating monochromator (Jobin Yvon Triax 180) with a resolution of 0.5 nm. The luminescence decay curves were measured by exciting the sample with a 10 ns optical parametric oscillator (OPO) laser (Ekspla NT342/3/UVE) sintonised at 975 nm. The signal was acquired by a digital oscilloscope (Tektronix 2430A) controlled by a personal computer. All measurements were made at room temperature and were corrected by the spectral response of the equipment.

3. Results and discussion

The upconverted luminescence spectrum was obtained under excitation of the co-doped sample with a cw laser diode at 980 nm. The result is shown in Fig. 1, in which three clear emissions of red, green and blue bands centred at around 650, 545 and 484 nm, respectively, can be observed. From the analysis of Fig. 1, the energy level diagram presented in Fig. 2 and previous works [32], it can be inferred that upconverted emissions corresponding to the 650 and 545 nm are caused by the $^4F_{9/2}\rightarrow{}^4I_{15/2}$ and $^4S_{3/2}(^2H_{11/2})\rightarrow{}^4I_{15/2}$ transitions, respectively, from Er^{3+} ions. The green emission can be separated into two bands, related to the $^2H_{11/2}\rightarrow{}^4I_{15/2}$ transition at 529 nm and the $^4S_{3/2}\rightarrow{}^4I_{15/2}$ transition, mentioned before at 545 nm. The multiplets observed can be associated, in principle, to the crystal field effect, causing degeneracy via stark-splitting of Er^{3+} energy levels. As Fig. 2 shows, initially, cw laser excitation at 980 nm populates resonantly, via ground state absorption (GSA), $^4I_{11/2}$ and $^2F_{5/2}$ levels of Er^{3+} and Yb^{3+} ions, respectively. From $^2F_{5/2}$ level of Yb^{3+} energy transfer can increase the population of $^4I_{11/2}$ level via $(^2F_{5/2},{}^4I_{15/2})\rightarrow(^2F_{7/2},{}^4I_{11/2})$ transitions. The $^4S_{3/2}(^2H_{11/2})$ emitting levels can be populated via $^4I_{11/2}$ by excited-state absorption of pump radiation (ESA) and/or energy transfer upconversion (labelled as ETU1) processes, involving a single or two excited Er^{3+} ions, respectively, or via an energy transfer upconversion (labelled as ETU2) process involving an Yb^{3+} ion. In an ESA process, the $^4F_{7/2}$ state is populated after the direct absorption of a second laser

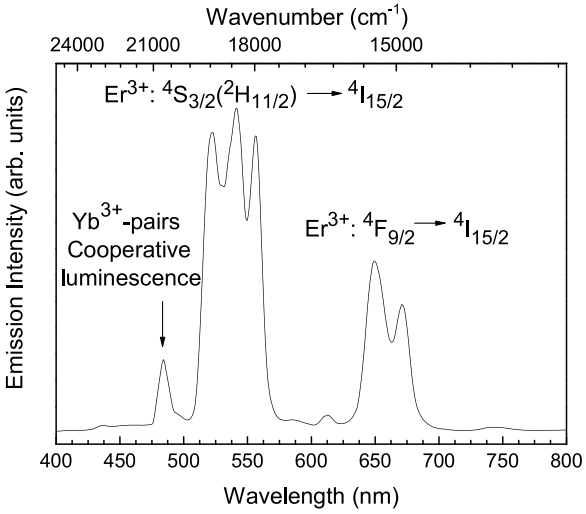

Fig. 1. Upconversion spectrum of $Y(BO_3)$: Er^{3+}-Yb^{3+} co-doped sample under cw laser diode excitation at 980 nm.

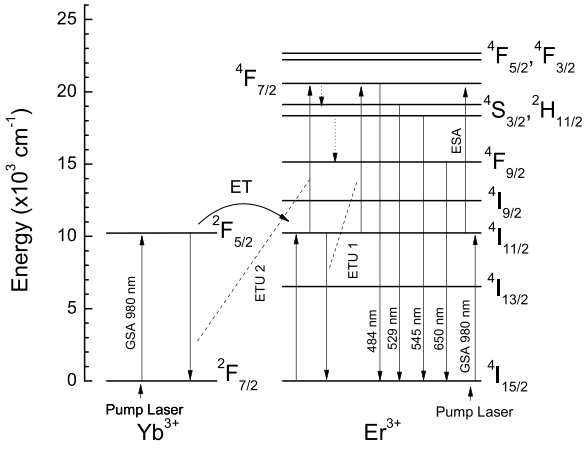

Fig. 2. Energy level diagrams of the Yb^{3+} and Er^{3+} ions showing possible excitation pathways and upconversion mechanisms.

photon while the Er^{3+} ion is still at the $^4I_{11/2}$ metastable level during the same laser pulse. Subsequent non-radiative relaxation, via lattice phonon in form of heat from the $^4F_{7/2}$ state, feeds the $^4S_{3/2}(^2H_{11/2})$ and $^4F_{9/2}$ emitting states. On the other hand, in an ETU1 process, one Er^{3+} ion is excited from the $^4I_{11/2}$ metastable level up to the $^4F_{7/2}$ level thanks to the energy transferred by another Er^{3+} ion in the $^4I_{11/2}$ intermediate level, that decays to the $^4I_{15/2}$ ground state, following the $(^4I_{11/2},{}^4I_{11/2})\rightarrow(^4F_{7/2},{}^4I_{15/2})$ scheme. For the ETU2 process, the $^4F_{7/2}$ state is populated after an energy transfer form an Yb^{3+} ion, according to the $(^2F_{5/2},{}^4I_{11/2})\rightarrow(^2F_{7/2},{}^4F_{7/2})$ process. It must be taken into account than the absorption cross-section of Yb^{3+} ions is much higher than the absorption cross-section of Er^{3+} ions, so the initial population process could be dominated by the energy transfer process from Yb^{3+} to Er^{3+}.

The last blue emission at 484 nm could be attributed to cooperative luminescence originated from coupled Yb^{3+}-Yb^{3+}states, impurities of Tm^{3+} ions or emissions from Er^{3+} ions. In the first case, emission involves neighbouring excited Yb^{3+} ion coupled states [$^2F_{5/2}$, $^2F_{5/2}$] giving raise to luminescence corresponding to twice the energy of the $^2F_{5/2}$ level. For the study of the cooperative luminescence emission, the energy level diagram for Yb^{3+}-pairs can be interpreted considering a weakly coupled model [33] with a three-energy-level structure (see Fig. 3). The first level, [$^2F_{7/2}$, $^2F_{7/2}$], is the ground state in which Yb^{3+} ions are not excited. The second level is degenerated, [$^2F_{5/2}$, $^2F_{7/2}$],

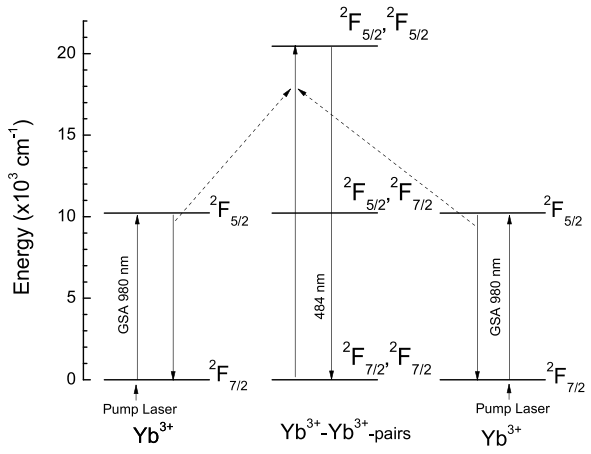

Fig. 3. Schematic energy level diagrams of the Yb^{3+} ions and Yb^{3+}-pairs. Lines show the Yb^{3+}-Yb^{3+} cooperative process.

[$^2F_{7/2}$, $^2F_{5/2}$], and corresponds to one Yb^{3+} ion in the ground state and another one excited. The third level, [$^2F_{5/2}$, $^2F_{5/2}$], is the situation in which two Yb^{3+} ions are excited in the $^2F_{5/2}$ level. In this model, the energy associated to the second level is the same as the energy of the $^2F_{5/2}$ state, whereas the energy of the third level corresponds to twice the $^2F_{5/2}$ level. Taking this scheme into account, two NIR photons from the third level can be produced via successive radiative transitions:

$$Yb(^2F_{5/2}) + Yb(^2F_{5/2}) \rightarrow Yb(^2F_{5/2}) + Yb(^2F_{7/2}) + h\nu \text{ (NIR)}$$

$$Yb(^2F_{5/2}) + Yb(^2F_{7/2}) \rightarrow Yb(^2F_{7/2}) + Yb(^2F_{7/2}) + h\nu \text{ (NIR)}$$

or one blue photon from the anti-Stokes emission as follows:

$$Yb(^2F_{5/2}) + Yb(^2F_{5/2}) \rightarrow Yb(^2F_{7/2}) + Yb(^2F_{7/2}) + h\nu \text{ (blue)}$$

In contrast to the cooperative luminescence case, the presence of Tm^{3+} impurities could be responsible for another way of blue emission. Although the starting Yb_2O_3 has 99.99 % purity given by the manufacturer, the presence of Tm^{3+} impurities, in the form of oxides as Tm_2O_3, cannot be ruled out in the first instance, and small amounts of impurities, even in the order of few ppm, can produce clear luminescence. In fact, the emission due to unexpected impurities has been reported before [34]. In this case, the energy transfer upconversion mechanism is a little bit more difficult because there are no Stark Tm^{3+} levels in resonance with both excitation at 980 nm and $^2F_{5/2} \rightarrow {}^2F_{7/2}$ transition of the Yb^{3+} ions. If the blue band was originated from Tm^{3+} ions, three photon absorption would be necessary to reach the $^1G_4$ emitting level [35–42] (see Fig. 4). This process can be described as a

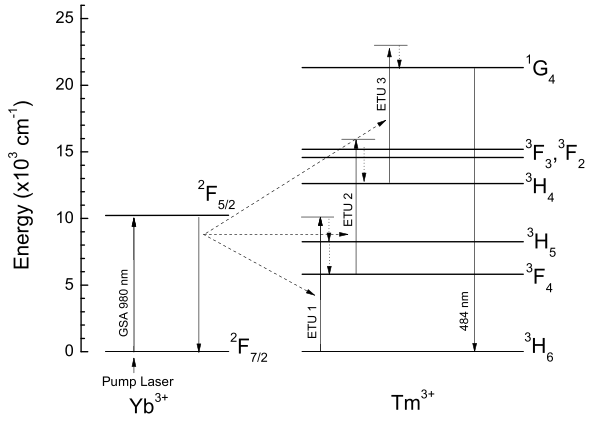

Fig. 4. Energy level diagrams of the Yb^{3+} and Tm^{3+} ions showing the energy transfer upconversion mechanism.

three-step exothermic phonon-assisted energy transfer. Under cw excitation at 980 nm, Yb^{3+} ions are promoted to the $^2F_{5/2}$ level. From this level, a non-resonant energy transfer to a nearest Tm^{3+} ion excites to $^3H_5$ level (ETU1) from which non-radiative relaxation feeds the lower $^3F_4$ level. From this level, one photon can be reabsorbed by energy transfer from Yb^{3+} ions, promoting Tm^{3+} ions to the $^3F_3$ level (ETU2), relaxing via multiphonon de-excitation to the $^3H_4$ level. Finally, a third non-resonant energy transfer from Yb^{3+} ions can populate the $^1G_4$ level (ETU3) from which the blue emission is produced according to $^1G_4 \rightarrow {}^3H_6$ transition. By contrast, in the case of cooperative luminescence, two simultaneously excited Yb^{3+} ions in the $^2F_{5/2}$ state are de-excited, emitting a single photon corresponding to the sum of the energy of the two electronic transitions.

In order to elucidate if this blue luminescence can be attributed to a cooperative process or emission fromTm^{3+} ions and, at the same time, to verify the above-described schemes for red and green emissions from Er^{3+} ions, the intensity of the upconverted signal on the incident pump power was measured and presented in Fig. 5. The upconversion emission intensity I_{em}, for an unsaturated process, is proportional to the n-th power of the incident pump laser power P_{pump} according to the following relation [43]:

$$I_{em} = (P_{pump})^n \quad (1)$$

where n is the number of photons involved in the population of the emitting level. The graphical representation of the integrated luminescence with respect to the pump power, in logarithmic scale for both axes, make it possible to obtain the number of photons through the slope of the curves after the linear fits to the data. The least square fit of the experimental results to Eq. (1) produces slopes of 1.02, 1.67 and 1.52 values for red, green and blue emissions, respectively. This quadratic dependence of the intensities on the pump power indicates two photons are responsible for populating the emitting levels. For red and green emissions, the dependence is in agreement with the potential processes described above [44,45]. Thus, the values obtained for n indicate an unsaturated regime with no saturation effect observed in relation to Yb^{3+} absorption or saturation of excited states of Er^{3+} ions [46]. With respect to the blue emission, according to this quadratic dependence, the signal originates from cooperative luminescence by Yb^{3+}-pairs [47,48]. The less than square dependence observed could be due to the presence of ETU mechanisms, in competition with cooperative luminescence. The emission from Tm^{3+} impurities can be ruled out because, as it was described above, three photons would be required to reach the $^1G_4$ emitting level. In fact, luminescence of a few ppm of Tm^{3+} may result in higher intensity than cooperative luminescence, which is a second-order

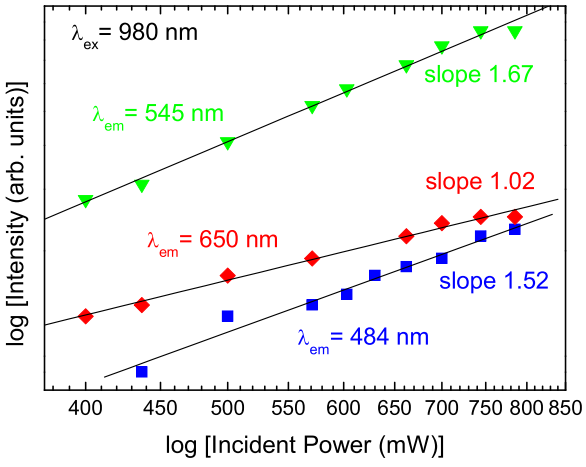

Fig. 5. Dependence of the integrated upconversion intensities as function of the incident pump power. The symbols represent the emission intensities at 484 nm (blue squares), 545 nm (green triangles) and 650 nm (red rhombus).

process. However, this result does not discriminate if the blue emission could be attributed to $^4F_{7/2} \rightarrow {}^4I_{15/2}$ transition from Er^{3+} ions, which also requires two photons.

Moreover, with the aim to confirm the cooperative effect, the decay curves of the 980 and 484 nm emissions were analysed. The dependence of the NIR and cooperative luminescence on Yb^{3+} concentration, for single-doped sample, can be determined by means of a rate equation model as follows [49,50]:

$$\frac{dN_2}{dt} = PN_1 - CN_2^2 - \frac{N_2}{\tau_2} \quad (2)$$

where N_1 and N_2 represent the population densities of the ground state ($^2F_{7/2}$) and the excited state ($^2F_{5/2}$) levels, respectively, P is the pumping rate, C is the cooperative luminescence rate constant, and τ_2 is the experimental lifetime of the NIR emission. The inverse or the term τ_2 can be interpreted as the sum radiative and non-radiative de-excitation. The term CN_2^2 indicates the loss in population of the excited state ($^2F_{5/2}$) level by the creation of Yb^{3+}-pairs. The NIR intensity can be determined by taking into account that it is proportional to N_2. Similarly, the cooperative intensity is proportional to N_2^2. In this sense, it can be proven that, for low doping concentration, the NIR and cooperative luminescence intensities can be expressed, respectively, as [27,51]:

$$I_{NIR} \propto N_2 \propto \exp\left(-\frac{t}{\tau_2}\right) \quad (3)$$

$$I_{CL} \propto N_2^2 \propto \exp\left(-\frac{t}{\tau_2/2}\right) \quad (4)$$

Fig. 6 shows the luminescence decay curves for 980 nm and 484 nm, corresponding to Yb^{3+}:$^2F_{5/2} \rightarrow {}^2F_{7/2}$ and cooperative luminescence, respectively, obtained under 975 nm laser pulsed excitation to the $^2F_{5/2}$ level of the Yb^{3+} ions. As can be seen, the kinetics present a non-exponential character with a fast initial decaying. This fast-decaying component observed in decay profiles can be related to both the energy transfer to Er^{3+} neighbouring ions and cooperative transfer to Yb^{3+} ions. In the second scenario, Yb^{3+} pairs would be responsible. Non-radiative de-excitation is not considered because the energy gap between Yb^{3+} levels is very large and multiphonon relaxation by vibrational phonons is negligible. In the case of quenching, the energy transfer would be from active ions to impurities present on the sample.

From these curves, the averages lifetimes have been calculated by using the following equation [52]:

$$<\tau> = \frac{\int_0^\infty I(t)tdt}{\int_0^\infty I(t)dt} \quad (5)$$

where τ is the effective decay time and $I(t)$ is the intensity at time t.

The lifetimes obtained are 1.5 μs and 4.9 μs for the 484 nm and 980 nm emissions, respectively. The average lifetime due to a cooperative process is expected to be about the half of the NIR emission, indicating a strong evidence of cooperative luminescence [28,53]. The discrepancy observed in our results is due to the decay curves not being exactly exponential (as can be seen in Fig. 6), which could be related to the energy transfer processes from Yb^{3+} to Er^{3+}. These energy transfers mechanisms are not considered in Eq. 2 and can be considered as being responsible for the slight lower life time value measured with respect to the expected value. However, the NIR intensity is proportional to the population of $^2F_{5/2}$ level ($N_{2_{F_{5/2}}}$) and the blue intensity of the virtual level which produces the emission at 484 nm is proportional to $(N_{2_{F_{5/2}}})^2$. This is illustrated in Fig. 6, observing a good agreement in the overlapping between the $(N_{2_{F_{5/2}}})^2$ (black line) and the 484 nm decay. Based on the kinetic discussions, and the power dependence of the emission, it can be concluded that the cooperative energy transfer between Yb^{3+} ions induces the cooperative luminescence. This result indicates that contributions from Tm^{3+} impurities or Er^{3+} ions can be excluded. Moreover, cooperative luminescence is an ideal signature of Yb^{3+} clustering in agreement with results obtained in other samples, for example, calcium aluminates [28], silica-based glasses [54] and alkaline-earth fluoride crystal [55]. From a structural point of view, cooperative luminescence is related to the Yb^{3+} pairing in Y^{3+} crystallographic sites. This process relies on Coulombian interaction between Yb^{3+} ions having a strong dependence on inter-ionic distances, confirming the clustering of Yb^{3+} ions in crystal.

The basic requirements for PDPs are stability and emission color purity. In the framework of the Commission Internationale de I'Eclairage (CIE) 1931, the XY chromaticity coordinate graph was plotted (see Fig. 7) for the study of the color purity of the sample. As can be seen, the CIE 1931 graph comprises a triangle of red, green and blue, where the position in the diagram is called the chromaticity point. The calculated x and y chromaticity coordinates are 0.29 and 0.64, respectively, corresponding to the green point in Fig. 7. As can be seen inset, an intense

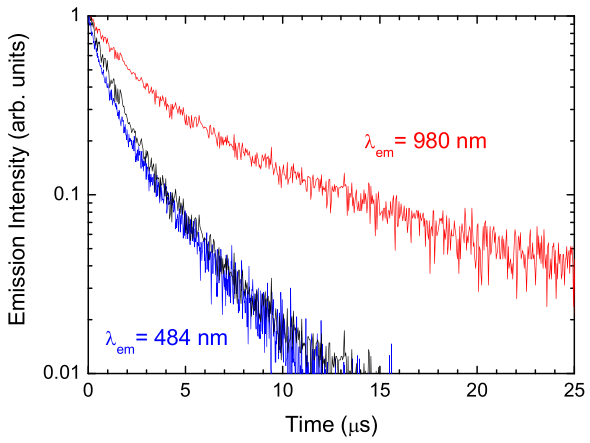

Fig. 6. Emission decay curves, under 975 nm laser pulsed excitation, of luminescence at 980 nm (red line) and cooperative luminescence at 484 nm (blue line). Black line represents the quadratic emission decay of 980 nm luminescence.

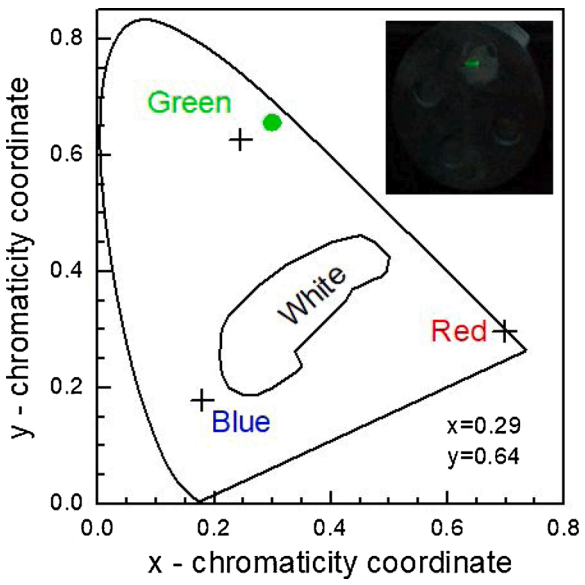

Fig. 7. Representation, on the CIE 1931 diagram, of chromaticity coordinates (green point) associated to the upconverted emissions. The inset corresponds to the image of the sample under cw laser excitation at 980 nm. In his image an intense green upconversion emission is observed.

green upconversion emission can be observed with the naked eye. This result indicates that a single infrared excitation makes it possible to obtain a green light color, whose coordinates are close to the values required for PDPs.

4. Conclusions

Upconversion to visible light has been obtained in the $Y(BO_3)$: Er^{3+}-Yb^{3+} co-doped sample, after cw NIR laser excitation at 980 nm. The upconverted emissions correspond to red, green and blue bands centred at around 650, 545 and 484 nm, respectively. The red and green emissions can be interpreted as the result of an effective energy transfer from Yb^{3+} to Er^{3+} ions. For the blue luminescence, the intensity of the upconverted signal on the incident pump power was studied, resulting in two photons being required to produce this emission. As was concluded, impurities as Tm^{3+} ions can be ruled out, the nature of this emission being a cooperative luminescence process associated to Yb^{3+}-pairs.

In the color diagram, the chromaticity coordinates obtained are $x = 0.29$ and $y = 0.64$, corresponding to a dominant green emission color purity, fulfilling the requirement for high quality PDPs. For future works, samples with different concentrations of Er^{3+} and Yb^{3+}, or including Tm^{3+} ions, could be synthesized in order to study the possibility of obtaining a tunable color display.

Declaration of Competing Interest

The authors report no declarations of interest.

References

[1] C.-H. Kim, I.-E. Kwon, C.-H. Park, Y.-J. Hwang, H.-S. Bae, B.-Y. Yu, C.-H. Pyun, G.-Y. Hong, ChemInform Abstract: Phosphors for Plasma Display Panels, J. Non. Cryst. Solids 311 (2000) 33–39, https://doi.org/10.1016/S0925-8388(00)00856-2.

[2] L. Chen, Y. Jiang, G. Yang, G. Zhang, X. Xin, D. Kong, New red phosphor (Y, Gd, Lu) BO3: Eu^{3+} for PDP applications, J. Rare Earths 27 (2009) 312–315, https://doi.org/10.1016/S1002-0721(08)60240-9.

[3] J. Li, Y. Wang, B. Liu, Influence of alkali metal ions doping content on photoluminescence of (Y, Gd) BO_3:Eu red phosphors under VUV excitation, J. Lumin. 130 (2010) 981–985, https://doi.org/10.1016/j.jlumin.2010.01.009.

[4] Y. Hao, Y. Wang, X. Hu, X. Liu, E. Liu, J. Fan, H. Miao, Q. Sun, YBO3: Ce^{3+}, Yb^{3+}based near-infrared quantum cutting phosphors: Synthesis and application to solar cells, Ceram. Int. 42 (2016) 9396–9401, https://doi.org/10.1016/j.ceramint.2016.02.158.

[5] Y. Noh, M. Choi, K. Kim, O. Song, Properties of working electrodes with nano YBO_3:Eu^{3+} phosphor in a dye sensitized solar cell, J. Korean Ceram. Soc. 53 (2016) 253–257, https://doi.org/10.4191/kcers.2016.53.2.253.

[6] L. Lou, D. Boyer, G. Bertrand-Chadeyron, E. Bernstein, R. Mahiou, J. Mugnier, Sol-gel waveguide thin film of YBO_3: preparation and characterization, Opt. Mater. (Amst). 15 (2000) 1–6, https://doi.org/10.1016/S0925-3467(00)00014-8.

[7] L. Chen, A.Q. Luo, Y. Zhang, X.H. Chen, H. Liu, Y. Jiang, S.F. Chen, K.J. Chen, H. C. Kuo, Y. Tao, G. Bin Zhang, The site-selective excitation and the dynamical electron-lattice interaction on the luminescence of YBO_3: Sb^{3+}, J. Solid State Chem. 201 (2013) 229–236, https://doi.org/10.1016/j.jssc.2013.02.034.

[8] C. Li, X. Du, Y. Shi, J. Huang, L. Jin, Z. Wang, X. Zhang, Carbon nanodots enhance and optimize the photoluminescence of micro-spherical YBO_3:Eu^{3+} phosphors, J. Alloys. Compd. 783 (2019) 813–819, https://doi.org/10.1016/j.jallcom.2018.12.383.

[9] I.E. Kwon, B.Y. Yu, H. Bae, Y.J. Hwang, T.W. Kwon, C.H. Kim, C.H. Pyun, S.J. Kim, Luminescence properties of borate phosphors in the UV/VUV region, J. Lumin. 87 (2000) 1039–1041, https://doi.org/10.1016/S0022-2313(99)00532-3.

[10] H. Hara, S. Takeshita, T. Isobe, Y. Nanai, T. Okuno, T. Sawayama, S. Niikura, Glycothermal synthesis and photoluminescent properties of Ce^{3+}-doped YBO_3 mesocrystals, J. Alloys. Compd. 577 (2013) 320–326, https://doi.org/10.1016/j.jallcom.2013.05.203.

[11] J.T. Ingle, R.P. Sonekar, S.K. Omanwar, Y. Wang, L. Zhao, Combustion synthesis and VUV photoluminescence studies of borate host phosphors YBO_3:RE^{3+} (RE = Eu^{3+}, Tb^{3+}) for PDPs applications, Combust. Sci. Technol. 186 (2014) 83–89, https://doi.org/10.1080/00102202.2013.846332.

[12] G. Jia, H. You, K. Liu, Y. Zheng, N. Guo, J. Jia, H. Zhang, Highly uniform YBO_3 hierarchical architectures: Facile synthesis and tunable luminescence properties, Chem. - A Eur. J. 16 (2010) 2930–2937, https://doi.org/10.1002/chem.200902834.

[13] F. Wen, W. Li, Z. Liu, T. Kim, K. Yoo, S. Shin, J.H. Moon, J.H. Kim, Hydrothermal synthesis of Sb^{3+} doped and (Sb^{3+}, Eu^{3+}) co-doped YBO_3 with nearly white light luminescence, Solid State Commun. 133 (2005) 417–420, https://doi.org/10.1016/j.ssc.2004.12.013.

[14] Y. Tian, B. Tian, B. Chen, C. Cui, P. Huang, L. Wang, R. Hua, Ionic liquid-assisted hydrothermal synthesis and excitation wavelength-dependent luminescence of YBO_3:Eu^{3+} nano-/micro-crystals, J. Alloys. Compd. 590 (2014) 61–67, https://doi.org/10.1016/j.jallcom.2013.12.098.

[15] G. Jia, P.A. Tanner, C.K. Duan, J. Dexpert-Ghys, Eu^{3+} spectroscopy: A structural probe for yttrium orthoborate phosphors, J. Phys. Chem. C. 114 (2010) 2769–2775, https://doi.org/10.1021/jp910329k.

[16] L. Jia, Z. Shao, Q. Lü, Y. Tian, J. Han, Preparation of red-emitting phosphor (Y,Gd) BO_3:Eu^{3+} by high temperature ball milling, Ceram. Int. 40 (2014) 739–743, https://doi.org/10.1016/j.ceramint.2013.06.063.

[17] K.A. Koparkar, N.S. Bajaj, S.K. Omanwar, Effect of partially replacement of Gd3+ ions on fluorescence properties of YBO_3:Eu^{3+} phosphor synthesized via precipitation method, Opt. Mater. (Amst). 39 (2015) 74–80, https://doi.org/10.1016/j.optmat.2014.11.001.

[18] W. Pan, P. Wang, Y. Xu, R. Liu, Electrodeposition and luminescent properties of YBO_3:Eu^{3+} and Y_3BO_6:Eu^{3+} films, Thin Solid Films 578 (2015) 69–75, https://doi.org/10.1016/j.tsf.2015.02.018.

[19] H. Zhu, L. Zhang, T. Zuo, X. Gu, Z. Wang, L. Zhu, K. Yao, Sol-gel preparation and photoluminescence property of YBO_3:Eu^{3+} /Tb^{3+} nanocrystalline thin films, Appl. Surf. Sci. 254 (2008) 6362–6365, https://doi.org/10.1016/j.apsusc.2008.03.183.

[20] A. Szczeszak, S. Lis, V. Nagirnyi, Spectroscopic properties of Eu^{3+} doped YBO_3 nanophosphors synthesized by modified co-precipitation method, J. Rare Earths 29 (2011) 1142–1146, https://doi.org/10.1016/S1002-0721(10)60613-8.

[21] V. Dubey, J. Kaur, S. Agrawal, N.S. Suryanarayana, K.V.R. Murthy, Effect of Eu^{3+} concentration on photoluminescence and thermoluminescence behavior of YBO_3:Eu^{3+} phosphor, Superlattices Microstruct. 67 (2014) 156–171, https://doi.org/10.1016/j.spmi.2013.12.026.

[22] H. Ogata, S. Takeshita, T. Isobe, T. Sawayama, S. Niikura, Factors for determining photoluminescence properties of YBO_3:Ce^{3+} phosphor prepared by hydrothermal method, Opt. Mater. (Amst). 33 (2011) 1820–1824, https://doi.org/10.1016/j.optmat.2011.07.003.

[23] L. Wang, L. Shi, N. Liao, H. Jia, P. Du, Z. Xi, L. Wang, D. Jin, Photoluminescence properties of Y_2O_3:Tb^{3+} and YBO_3:Tb^{3+} green phosphors synthesized by hydrothermal method, Mater. Chem. Phys. 119 (2010) 490–494, https://doi.org/10.1016/j.matchemphys.2009.10.002.

[24] M.O. Onani, J.O. Okil, F.B. Dejene, Solution-combustion synthesis and photoluminescence properties of YBO_3:Tb^{3+} phosphor powders, Phys. B Condens. Matter 439 (2014) 133–136, https://doi.org/10.1016/j.physb.2013.10.056.

[25] X. Zhang, Z. Zhao, X. Zhang, A. Marathe, D.B. Cordes, B. Weeks, J. Chaudhuri, Tunable photoluminescence and energy transfer of YBO_3:Tb^{3+}, Eu^{3+} for white light emitting diodes, J. Mater. Chem. C. 1 (2013) 7202–7207, https://doi.org/10.1039/c3tc31200c.

[26] K. Das, A. Marathe, X. Zhang, Z. Zhao, J. Chaudhuri, Superior white light emission and color tunability of tri-doped YBO_3:Tb^{3+}, Eu^{3+} and Dy^{3+} for white light emitting diodes, RSC Adv. 6 (2016) 95055–95061, https://doi.org/10.1039/c6ra18217h.

[27] B. Schaudel, P. Goldner, M. Prassas, F. Auzel, Cooperative luminescence as a probe of clustering in Yb^{3+} doped glasses, J. Alloys. Compd. 300 (2000) 443–449, https://doi.org/10.1016/S0925-8388(99)00760-4.

[28] M. Puchalska, M. Sobczyk, J. Targowska, A. Watras, E. Zych, Infrared and cooperative luminescence in Yb^{3+} doped calcium aluminate $CaAl_4O_7$, J. Lumin. 143 (2013) 503–509, https://doi.org/10.1016/j.jlumin.2013.05.020.

[29] Z. Pan, A. Ueda, R. Mu, S.H. Morgan, Upconversion luminescence in Er^{3+}-doped germanate-oxyfluoride and tellurium-germanate-oxyfluoride transparent glass-ceramics, J. Lumin. 126 (2007) 251–256, https://doi.org/10.1016/j.jlumin.2006.07.021.

[30] Z. Hu, Y. Wang, E. Ma, D. Chen, F. Bao, Microstructures and upconversion luminescence of Er^{3+} doped and Er^{3+}/Yb^{3+} co-doped oxyfluoride glass ceramics, Mater. Chem. Phys. 101 (2007) 234–237, https://doi.org/10.1016/j.matchemphys.2006.04.001.

[31] P. Haro-González, F. Rivera-López, I.R. Martín, a.D. Lozano-Gorrín, C. González-Silgo, V.M. Sánchez-Fajardo, C. Guzmán-Afonso, M.E. Torres, Second harmonic generation in Er^{3+}–Yb^{3+}:YBO_3, Mater. Lett. 64 (2010) 650–653, https://doi.org/10.1016/j.matlet.2009.12.016.

[32] C. Yu, J. Zhang, L. Wen, Z. Jiang, New transparent Er^{3+}-doped oxyfluoride tellurite glass ceramic with improved near infrared and up-conversion fluorescence properties, Mater. Lett. 61 (2007) 3644–3646, https://doi.org/10.1016/j.matlet.2006.12.006.

[33] X. Qiao, T. Tsuboi, Excimer-like Yb^{3+}-pair and photoluminescence spectra of Yb^{3+}-molybdates, J. Alloys. Compd. 724 (2017) 520–527, https://doi.org/10.1016/j.jallcom.2017.07.062.

[34] R. Ternane, M. Ferid, Y. Guyot, M. Trabelsi-Ayadi, G. Boulon, Luminescent properties of Yb-doped monoclinic yttrium polyphosphates, J. Lumin. 128 (2008) 387–393, https://doi.org/10.1016/j.jlumin.2007.09.007.

[35] R. Lisiecki, G. Dominiak-Dzik, W. Ryba-Romanowski, I. Földvári, Á. Péter, Energy transfer and up-conversion in Bi_2TeO_5 crystals co-doped with Yb^{3+} and Tm^{3+}, Opt. Mater. (Amst). 31 (2008) 306–310, https://doi.org/10.1016/j.optmat.2008.04.016.

[36] Y. Liu, C. Xu, Q. Yang, White upconversion of rare-earth doped ZnO nanocrystals and its dependence on size of crystal particles and content of Yb^{3+} and Tm^{3+}, J. Appl. Phys. 105 (2009) 1–6, https://doi.org/10.1063/1.3088881.

[37] Y. Yang, Y. Chu, Z. Chen, Y. Ma, L. Liao, H. Li, J. Peng, N. Dai, J. Li, L. Yang, Blue upconversion luminescence for Yb^{3+}/Tm^{3+} co-doped borosilicate glasses, J. Lumin. 195 (2018) 247–251, https://doi.org/10.1016/j.jlumin.2017.11.035.

[38] J. Tang, M. Yu, E. Wang, C. Ge, Z. Chen, Intense ultraviolet upconversion luminescence from YF_3: Yb/Tm submicrorice, Mater. Chem. Phys. 207 (2018) 530–533, https://doi.org/10.1016/j.matchemphys.2018.01.017.
[39] P.V. Dos Santos, M.V.D. Vermelho, E.A. Gouveia, M.T. De Araújo, A.S. Gouveia-Neto, F.C. Cassanjes, S.J.L. Ribeiro, Y. Messaddeq, Blue cooperative luminescence in Yb^{3+}-doped tellurite glasses excited at 1.064 μm, J. Chem. Phys. 116 (2002) 6772–6776, https://doi.org/10.1063/1.1463397.
[40] Y. Wei, F. Lu, X. Zhang, D. Chen, Synthesis and characterization of efficient near-infrared upconversion Yb and Tm codoped $NaYF_4$ nanocrystal reporter, J. Alloys. Compd. 427 (2007) 333–340, https://doi.org/10.1016/j.jallcom.2006.03.014.
[41] W. Huang, M. Ding, H. Huang, C. Jiang, Y. Song, Y. Ni, C. Lu, Z. Xu, Uniform $NaYF_4$:Yb, Tm hexagonal submicroplates: Controlled synthesis and enhanced UV and blue upconversion luminescence, Mater. Res. Bull. 48 (2013) 300–304, https://doi.org/10.1016/j.materresbull.2012.10.031.
[42] L. Liu, F. Qin, H. Zhao, T. Lv, Z. Zhang, W. Cao, Facile synthesis and upconversion luminescence of β-$NaYF_4$:Yb, Tm nanocrystals with highly tunable and uniform β-$NaYF_4$ shells, J. Alloys. Compd. 684 (2016) 211–216, https://doi.org/10.1016/j.jallcom.2016.04.302.
[43] M. Pollnau, D. Gamelin, S. Lüthi, H. Güdel, M. Hehlen, Power dependence of upconversion luminescence in lanthanide and transition-metal-ion systems, Phys. Rev. B - Condens. Matter Mater. Phys. 61 (2000) 3337–3346, https://doi.org/10.1103/PhysRevB.61.3337.
[44] Y. Zhang, H. Lei, G. Li, L. Zeng, J. Tang, Yb^{3+}/Er^{3+} co-doped transparent tellurite glass-ceramic for enhanced upconversion luminescence, Opt. Mater. (Amst) 99 (2020), 109552, https://doi.org/10.1016/j.optmat.2019.109552.
[45] L.Q. Minh, T.K. Anh, N.D. Hung, P.T. Minh Chau, N.T. Quy Hai, H. Van Tuyen, V. T. Thai Ha, V.D. Tu, W. Strek, Upconversion luminescence of $Gd_2O_3:Er^{3+}$ and $Gd_2O_3:Er^{3+}$/silica nanophosphors fabricated by EDTA combustion method, J. Rare Earths 37 (2019) 1126–1131, https://doi.org/10.1016/j.jre.2019.04.004.
[46] C. Jacinto, M.V.D. Vermelho, E.A. Gouveia, M.T. De Araujo, P.T. Udo, N.G. C. Astrath, M.L. Baesso, Pump-power-controlled luminescence switching in Yb^{3+} Tm^{3+} codoped water-free low silica calcium aluminosilicate glasses, Appl. Phys. Lett. 91 (2007) 2007–2009, https://doi.org/10.1063/1.2771051.
[47] X. Chen, Z. Song, Strong cooperative upconversion luminescence of ytterbium doped oxyfluoride nanophase vitroceramics, Solid State Commun. 136 (2005) 313–317, https://doi.org/10.1016/j.ssc.2005.08.019.
[48] G. Yao, Y. Cheng, F. Wu, X. Xu, L. Su, J. Xu, Spectral investigation of Yb-doped calcium pyroniobate crystal, J. Cryst. Growth 310 (2008) 725–730, https://doi.org/10.1016/j.jcrysgro.2007.11.106.
[49] V.D. Cacho, L.R.P. Kassab, S.L. Oliveira, R.D. Mansano, P. Verdonck, Blue cooperative luminescence properties in Yb^{3+} doped GeO_2-PbO-Bi_2O_3 vitreous system for the production of thin films, Thin Solid Films 515 (2006) 764–767, https://doi.org/10.1016/j.tsf.2005.12.176.
[50] K. Xiao, Z. Yang, Blue cooperative luminescence in Yb^{3+}-doped barium gallogermanate glass excited at 976 nm, J. Fluoresc. 16 (2006) 755–759, https://doi.org/10.1007/s10895-006-0134-4.
[51] L. Zhang, J. Yang, Z. Zhang, H. Yu, W. Pan, Blue cooperative up-conversion luminescence of Yb:Y_2O_3 transparent ceramics, Ceram. Int. 45 (2019) 9278–9282, https://doi.org/10.1016/j.ceramint.2019.02.006.
[52] T. Grzyb, K. Kubasiewicz, A. Szczeszak, S. Lis, Energy migration in $YBO_3:Yb^{3+},Tb^{3+}$ materials: Down- and upconversion luminescence studies, J. Alloys. Compd. 686 (2016) 951–961, https://doi.org/10.1016/j.jallcom.2016.06.230.
[53] X. Qiao, Y. Ye, Novel blue cooperative up-conversion luminescence of fully concentrated Yb-based $LiYb(MoO_4)_2$ phosphor, Mater. Lett. 161 (2015) 248–250, https://doi.org/10.1016/j.matlet.2015.08.113.
[54] E.A. Savel'ev, A.V. Krivovichev, V.O. Yapaskurt, K.M. Golant, Luminescence of Yb^{3+} ions in silica-based glasses synthesized by SPCVD, Opt. Mater. (Amst). 64 (2017) 427–435, https://doi.org/10.1016/j.optmat.2017.01.016.
[55] T. Aidilibike, J. Guo, Y. Li, X. Liu, W. Qin, Triplet cooperative luminescence of Yb^{3+}-doped AF_2 (A=Ca, Sr) crystals, J. Lumin. 188 (2017) 107–111, https://doi.org/10.1016/j.jlumin.2017.03.069.